JOURNAL OF NATURAL PRODUCTS

Article

Cite This: J. Nat. Prod. XXXX, XXX, XXX−XXX

pubs.acs.org/jnp

Synthesis of [3,3-$^2H_2$]-Dihydroartemisinic Acid to Measure the Rate of Nonenzymatic Conversion of Dihydroartemisinic Acid to Artemisinin

Kaitlyn Varela, Hadi D. Arman, and Francis K. Yoshimoto*

Department of Chemistry, The University of Texas at San Antonio, San Antonio, Texas 78249-0698, United States

Supporting Information

ABSTRACT: Dihydroartemisinic acid is the biosynthetic precursor to artemisinin, the endoperoxide-containing natural product used to treat malaria. The conversion of dihydroartemisinic acid to artemisinin is a cascade reaction that involves C−C bond cleavage, hydroperoxide incorporation, and polycyclization to form the endoperoxide. Whether or not this reaction is enzymatically controlled has been controversial. A method was developed to quantify the nonenzymatic conversion of dihydroartemisinic acid to artemisinin using LC-MS. A seven-step synthesis of 3,3-dideuterodihydroartemisinic acid (**23**) was accomplished beginning with dihydroartemisinic acid (**1**). The nonenzymatic rates of formation of 3,3-dideuteroartemisinin (**24**) from 3,3-dideuterodihydroartemisinic acid (**23**) were 1400 ng/day with light and 32 ng/day without light. Moreover, an unexpected formation of nondeuterated artemisinin (**3**) from 3,3-dideuterodihydroartemisinic acid (**23**) was detected in both the presence and absence of light. This formation of nondeuterated artemisinin (**3**) from its dideuterated precursor (**23**) suggests an alternative mechanistic pathway that operates independent of light to form artemisinin, involving the loss of the two C-3 deuterium atoms.

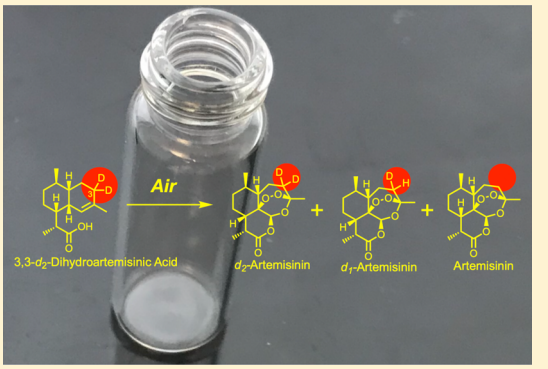

Artemisinin is the endoperoxide-containing natural product used to treat malaria.[1] Dihydroartemisinic acid is the biosynthetic precursor to artemisinin.[2] The conversion of dihydroartemisinic acid to artemisinin has been controversial in regard to whether or not the transformation is enzymatic in *Artemisia annua*, with evidence supporting both an enzymatic process[3−5] and a nonenzymatic process.[6,7] Our results confirmed the spontaneous, nonenzymatic conversion of dihydroartemisinic acid to artemisinin (Figure 1, **1** to **3**). Subsequently, a method was developed to quantify the rate of conversion of dihydroartemisinic acid to artemisinin using an internal standard to quantify product formation via an LC-MS method.

Dihydroartemisinic acid, which was isolated from *A. annua*,[2] is believed to be the biosynthetic precursor to artemisinin (**3**), the endoperoxide-containing natural product used to treat malaria (Figure 1). Dihydroartemisinic acid (**1**) was previously converted to artemisinin in the presence and absence of chlorophyll A; the production of artemisinin was reported as a percentage of conversion.[2] The endoperoxide of artemisinin is what confers its antimalarial activity, and therefore, many studies have developed methods to efficiently convert dihydroartemisinic acid to artemisinin.[8−10] The isolation of dihydroartemisinic acid hydroperoxide (**2**) from *A. annua* has been reported,[11] suggesting that this hydroperoxide is an intermediate to endoperoxide formation (**2** to **3**). Dihydroartemisinic acid hydroperoxide (**2**) can also be formed by treating dihydroartemisinic acid with singlet oxygen, i.e., irradiating a CH_2Cl_2 solution of dihydroartemisinic acid in the presence of methylene blue and O_2.[12] This resulting hydroperoxide has been shown to convert to artemisinin (**2** to **3**) over 4 days in 17% yield.[12] In a mechanistic study related to the conversion of dihydroartemisinic acid hydroperoxide to artemisinin (**2** to **3**), in trifluoroacetic acid/petroleum ether medium yielded 25% of artemisinin.[13] Both dihydroartemisinic acid and its hydroperoxide have been shown to convert to artemisinin (**1** to **3** and **2** to **3**) in $CDCl_3$ when each starting material was stored in an NMR tube over extended periods of time ("several weeks").[6] The rate of formation of artemisinin was reported as a percentage through integration of the ^1H NMR signals. Additionally, no raw NMR spectroscopic data of the compounds have been reported of this time course monitoring the conversion of dihydroartemisinic acid into artemisinin.[6]

Major efforts have been made to identify the endoperoxide forming enzyme in *A. annua*.[4,5] Artemisinin is found primarily in the glandular trichomes of *A. annua*. Proteomic[4] and transcriptomic[5] studies have identified the abundance of a peroxidase protein and mRNA, suggesting that this peroxidase is the enzyme that converts dihydroartemisinic acid to artemisinin. Other studies using recombinant expression of

Received: July 26, 2019

DOI: 10.1021/acs.jnatprod.9b00686
J. Nat. Prod. XXXX, XXX, XXX−XXX

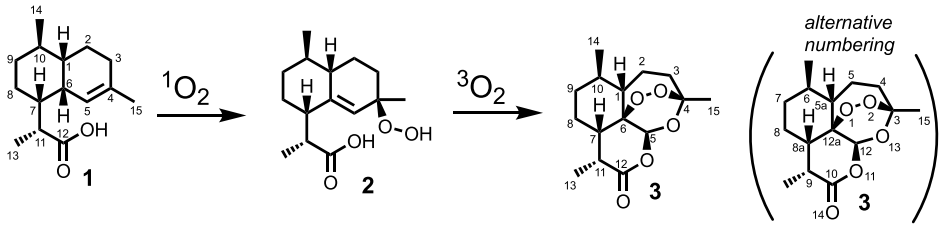

Figure 1. Formation of artemisinin (**3**) from dihydroartemisinic acid (**1**) through an allylic hydroperoxide intermediate (**2**). The numbering shown in structure **3** is the numbering system based on the carbon backbone in dihydroartemisinic acid (**2**), as has been previously reported,[14] and shown in parentheses is the alternative numbering for artemisinin.[13] To avoid confusion, the results from this article (Figure 4) will refer to the numbering system shown in the former structure.[14]

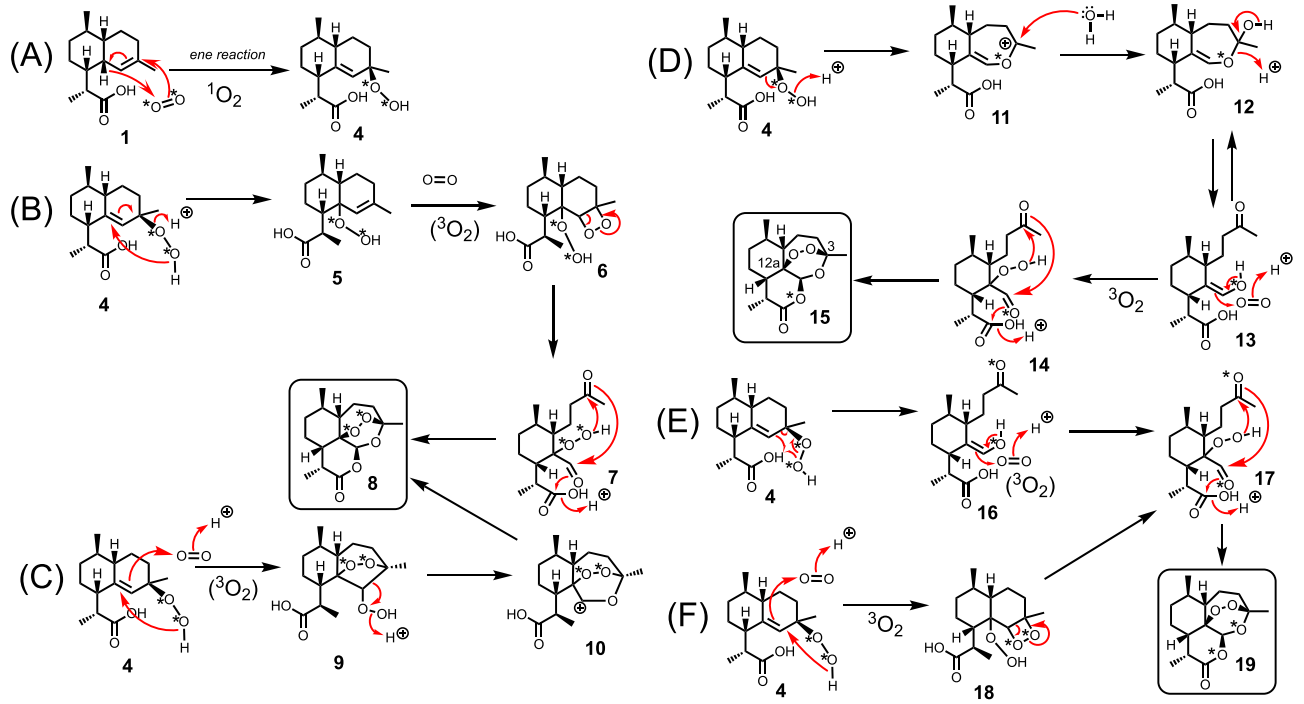

Figure 2. Dihydroartemisinic acid is converted to its hydroperoxide in the presence of singlet oxygen (A, **1** to **4**). The mechanisms of endoperoxide formation from dihydroartemisinic acid hydroperoxide (B–F). Mechanisms B and C were ruled out in a previous study[13] when dihydroartemisinic acid hydroperoxide (**4**) in the presence of $^{18}O_2$ gas confirmed that the oxygens in the endoperoxide bridge did not come from singlet oxygen. Instead, the source of these oxygens is triplet oxygen.

peroxidase of *A. annua* have shown the inability to convert artemisinic acid to artemisinin on its own, but this reaction was enabled when plant tissue was added.[3] Although these studies suggest the possibility of the existence of an endoperoxide forming enzyme (i.e., conversion of **1** to **3**, Figure 1), the nonenzymatic formation[6,7,13] of the endoperoxide in artemisinin has also been reported (vide infra).

Because the endoperoxide moiety of artemisinin confers its antimalarial properties, how the endoperoxide bridge is formed from dihydroartemisinic acid has been a topic of interest for decades. The first step is thought to involve an ene reaction with singlet oxygen to form dihydroartemisinic acid hydroperoxide (Figure 2A, **1** to **4**). The subsequent steps involve the C–C bond cleavage step and reaction with triplet oxygen to form the peroxide intermediate, which cyclizes to form artemisinin (shown in Figures 2B–F). In a study that involved the use of $^{18}O_2$-gas and the dihydroartemisinic acid hydroperoxide in the presence of acid in Et_2O,[13] ^{13}C NMR spectroscopy was used to analyze the carbon signals of the formed artemisinin. The significant upfield shift of C-3 and C-12a (C-4 and C-6 of **3** in Figure 1) confirmed that the endoperoxide oxygen comes from molecular oxygen reacting with the hydroperoxide intermediate (Figures 2D, E, and F). This observation rules out mechanisms B and C (Figures 2B and C), where the oxygens in the endoperoxide bridge come from the hydroperoxide oxygens (Figure 2, **8**). Mechanisms D, E, and F (Figure 2D, E, and F) show that the oxygen atoms in the endoperoxide bridge (Figure 2D–F, **15** and **19**) come from molecular oxygen when starting with dihydroartemisinic acid hydroperoxide (Figure 2D–F, **4**). Mechanism D shows a ring expansion of the hydroperoxide intermediate (Figure 2D, **4**) to form an initial oxocarbocation (**11** via Hock cleavage[15]), which is hydrated to form a hemiketal **12**. The hemiketal is in equilibrium with the acyclic enolic carbonyl isomer (**13**). This intermediate is reacting with triplet oxygen to form the hydroperoxide **14**, which cyclizes to form the endoperoxide **15**. Mechanism E shows a homolytic cleavage of the C-4–C-5 bond to directly form intermediate **16**. Mechanism F shows the formation of a dioxetane intermediate (Figure 2F, **18**) and simultaneous attack of triplet oxygen.[13] The dioxetane rearranges to intermediate **17**, which cyclizes to form endoperoxide **19**. Based on previous $^{18}O_2$ studies with

DOI: 10.1021/acs.jnatprod.9b00686
J. Nat. Prod. XXXX, XXX, XXX–XXX

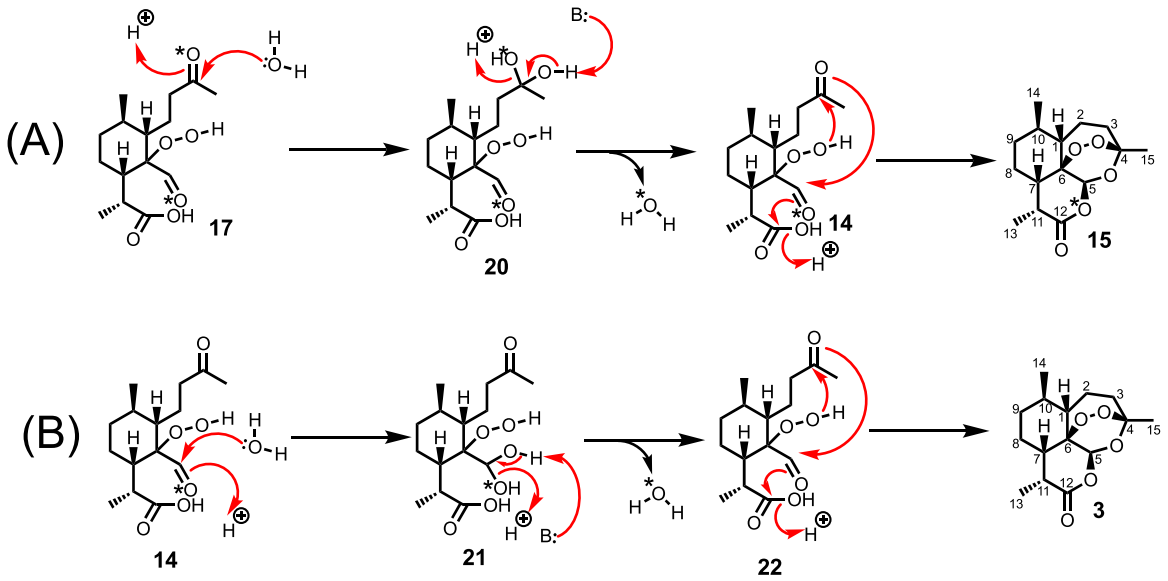

Figure 3. Explanation of the observation of a mixture of unlabeled and mono-^{18}O-incorporated artemisinin products consistent with the mechanisms shown in Figure 2E and F. (A) Formation of the *gem*-diol at the ketocarbonyl group (**20**) to result in the loss of its ^{18}O atom group. (B) Formation of the *gem*-diol at the formyl group (**21**) to result in the loss of its ^{18}O atom (**14** to **22**).

dihydroartemisinic acid hydroperoxide,[13] the resulting artemisinin product had a distribution of nonlabeled, monolabeled, and dilabeled products (with ^{18}O atoms) in a ratio of 53:100:43 as determined by mass spectrometry and 65:100:48, which was determined by ^{13}C NMR spectroscopy.[13] The observation that two ^{18}O atoms are incorporated into artemisinin only supports mechanisms E and F (Figure 2). The formation of monolabeled and unlabeled artemisinin products could be explained by the fact that the carbonyl oxygens of intermediates **17** and **14** (Figure 3) exchange with water in the medium (Figure 3A and B), resulting in the loss of the ^{18}O atoms in the carbonyl functional groups.

Despite extensive mechanistic studies of endoperoxide formation in artemisinin from dihydroartemisinic hydroperoxide, the biosynthetic conversion of dihydroartemisinic acid to artemisinin (Figure 1, **1** to **3**) has remained controversial (vide supra). Although singlet oxygen has been shown to be the source of hydroperoxide functionality (Figure 2A, **1** to **4**)[13] and is subsequently transformed into artemisinin in acidic medium, there has also been evidence of direct conversion of dihydroartemisinic acid to artemisinin (Figure 1, **1** to **3**) after storage of dihydroartemisinic acid in the freezer (−20 °C) in the absence of light for six months.[7]

The purpose of this investigation was to develop a method to quantify the rate of spontaneous formation of artemisinin from dihydroartemisinic acid (Figure 1, **3** from **1**). Initial pilot studies involved monitoring artemisinin production through ^{1}H NMR spectroscopy (Figure 4). Monitoring the reaction by ^{1}H NMR spectroscopy resulted in the observation of artemisinin formation through the appearance of the C-5-acetal proton at δ 5.88 ppm, but the signal-to-noise ratio was too low to measure an accurate amount of artemisinin (Figure 4 and Supporting Information). Therefore, we synthesized a 3,3-dideuterodihydroartemisinic acid isotopologue (Figure 5, **23**) and monitored the formation of 3,3-dideuteroartemisinin (**24**) while using nondeuterated artemisinin as an internal standard. The use of an internal standard with a known amount of artemisinin permitted the quantification of artemisinin formation through LC-HRMS data.

RESULTS AND DISCUSSION

NMR Experiment to Qualitatively Monitor the Rate of Conversion from Dihydroartemisinic Acid to Artemisinin. In order to firmly establish conditions of spontaneous conversion of dihydroartemisinic acid to artemisinin (**1** to **3**), a time course experiment was performed (Figure 4). Dried aliquots of dihydroartemisinic acid in either clear glass vials or amber glass vials were stored and open to air for different periods of time. The clear glass vials were exposed to sunlight, and the amber vials were stored in a dark cabinet.

The time course experiments using NMR spectroscopy confirmed the spontaneous formation of artemisinin from dihydroartemisinic acid when dihydroartemisinic acid was stored in vials open to air (Figure 4). Interestingly, the expected chemical shift for dihydroartemisinic acid hydroperoxide (H-5 proton should appear at δ 5.26)[11] possibly appeared at the 10-day time point (δ 5.24, slightly upfield of the satellite peak of H-5 proton of dihydroartemisinic acid). However, the area of this peak was insignificant relative to the proton of artemisinin (δ 5.88) and did not exactly match the expected chemical shift of dihydroartemisinic acid hydroperoxide. Furthermore, a proton with a chemical shift of δ 5.64 was present (Figure 4B, circled peak at the 7-day time point). This proton with a chemical shift of δ 5.64 matches the chemical shift of the vinyl proton of dihydro-*epi*-deoxyarteannuin B (Figure 4D, **X**).[16] Furthermore, in a previous study, which involved the long-term storage of a solution of dihydroartemisinic acid (**1**) in $CDCl_3$, dihydroartemisinic acid (**1**) was converted to dihydro-*epi*-deoxyarteannuin B (**X**).[6] As suggested previously,[6] dihydro-*epi*-deoxyarteannuin B (**X**) is formed from an intramolecular S_N2' displacement of hydrogen peroxide by the carboxylic acid moiety in dihydroartemisinic acid hydroperoxide (**2**). The mechanism of the intramolecular S_N2' displacement of hydrogen peroxide to form dihydro-*epi*-deoxyarteannuin B (**X**) is shown in Figure 4D.

In this time course (Figure 4), the detection of artemisinin (**3**) was confirmed by the presence of the hemiacetal proton at δ 5.88. Although other diagnostic peaks of artemisinin were

DOI: 10.1021/acs.jnatprod.9b00686
J. Nat. Prod. XXXX, XXX, XXX−XXX

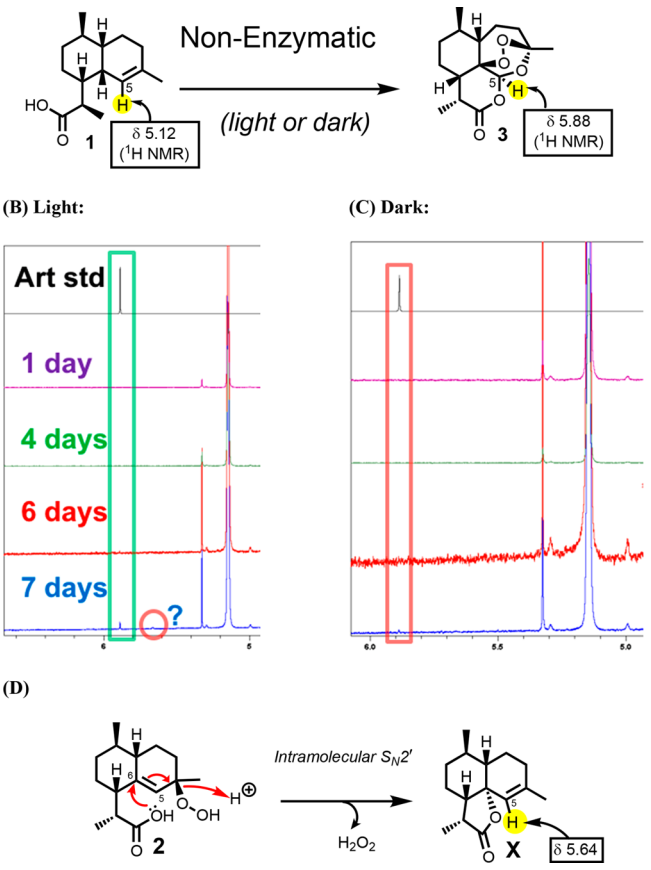

Figure 4. (A) Time course of spontaneous conversion of dihydroartemisinic acid (**1**) to artemisinin (**3**). ^{1}H NMR spectra overlay of time course experiment in (B) the light and (C) the dark. The hemiacetal proton of artemisinin appears at δ 5.88. The vinylic proton of dihydroartemisinic acid appears at δ 5.12 in $CDCl_3$ solvent at 500 MHz. A time point of zero days and no artemisinin was detected at δ 5.88 (the NMR sample was prepared immediately after the dried compound was dissolved in 0.7 mL of $CDCl_3$) (Supporting Information). (D) Mechanism of the possible formation of dihydro-*epi*-deoxyarteannuin B (**X**) from dihydroartemisinic acid hydroperoxide (**2**) through an intramolecular S_N2' displacement of H_2O_2 by the carboxylic acid nucleophile, which could explain the observation of the chemical shift at δ 5.64 (circled peak in Figure 4B).

present (e.g., multiplet at δ 3.5), the integration of these proton signals relative to dihydroartemisinic acid was small (i.e., the ratio of the integrals of the hemiacetal proton of artemisinin to the vinylic proton of dihydroartemisinic acid, which appears at δ 5.12, was 1 to ~100). The significant difference in relative peak areas between artemisinin and dihydroartemisinic acid coupled with the low signal-to-noise level of the methine proton of artemisinin (δ 5.88) made it difficult to accurately quantify the formation of artemisinin (i.e., Figure 4B and C). Nonetheless, this set of time course experiments using ^{1}H NMR spectroscopy was helpful in approximating the time to detect a significant amount of artemisinin formation when a dried sample of dihydroartemisinic acid was left open to air. Artemisinin formation from dihydroartemisinic acid (**3** from **1**) was clearly detected at 7 days with the appearance of the C-5-methine proton at δ 5.88 (Figure 4B). Moreover, another time course was performed, which involved dissolving dihydroartemisinic acid (**1**) in $CDCl_3$ and acquiring the ^{1}H NMR spectra at various time points (Supporting Information). Artemisinin was eventually formed but at a slower rate (i.e., no artemisinin was detected after 11 days). When artemisinin was detected (day 32 and day 35), a number of other peaks were also detected, suggesting decomposition of the parent compound (**1**) to a complex mixture (Supporting Information). In contrast, the dry conditions used in Figure 4 showed primarily artemisinin as the main product without decomposition to other products. However, the signal-to-noise level of the peak corresponding to artemisinin was not high enough to quantitatively measure the rate of artemisinin production (Figure 4B and C).

Therefore, in order to quantify the conversion of dihydroartemisinic acid to artemisinin (**1** to **3**), we were interested in developing a new method to measure the rate of formation of artemisinin from dihydroartemisinic acid using an LC-MS method and an internal standard (Figure 5). This strategy involved the synthesis of dideuterated dihydroartemisinic acid (Figure 5, **23**). To measure the rate of conversion from dihydroartemisinic acid to artemisinin, the 3,3-dideuterated dihydroartemisinic acid isotopologue would undergo (i) a time course involving a dried sample of dideuterated dihydroartemisinic acid (**23**) open to air in a vial to allow for spontaneous formation of dideuterated artemisinin (**24**), (ii) an extraction protocol involving the addition of an internal standard with a known amount of nondeuterated artemisinin (**3**), and (iii) analysis of d_2- and d_0-artemisinin by an LC-HRMS method (Figure 5).

Chemical Synthesis of 3,3-Dideuterodihydroartemisinic Acid (23) from Dihydroartemisinic Acid (1). The retrosynthetic analysis of 3,3-dideuterodihydroartemisinic acid (Figure 6, **23**) involves the incorporation of the two deuteriums at the C-3-position of an enone intermediate (Figure 6, **25**). This enone intermediate (**25**) would be derived from commercially available dihydroartemisinic acid (Figure 6, **1**), where the C12-carboxylic acid would be masked with a protecting group and the C-3-position would be oxidized at the C-3-position to yield the C-3-ketone (**25**).

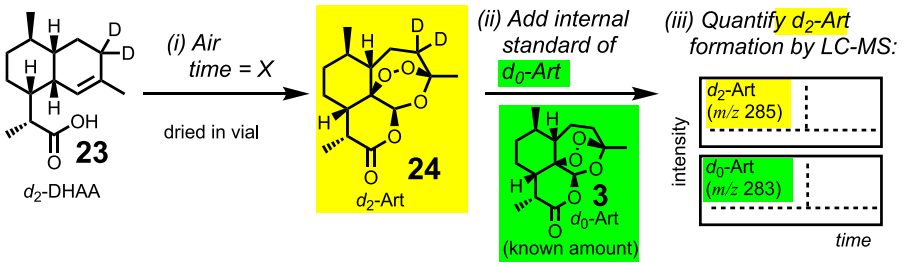

Figure 5. Schematic showing the use of 3,3-d_2-dihydroartemisinic acid (**23**) to measure the rate of nonenzymatic conversion to d_2-artemisinin (**24**) using d_0-artemisinin (**3**) as the internal standard.

DOI: 10.1021/acs.jnatprod.9b00686
J. Nat. Prod. XXXX, XXX, XXX−XXX

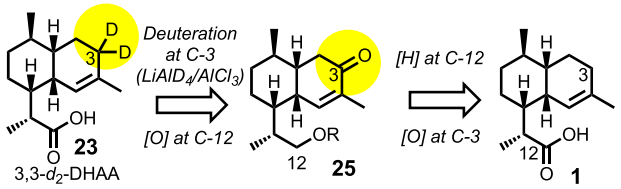

Figure 6. Retrosynthetic analysis of 3,3-dideuterodihydroartemisinic acid (**23**) from dihydroartemisinic acid (**1**).

The allylic oxidation at C-3 of artemisinic acid to yield 3-hydroxyartemisinic acid is known.[14] In the previous study, Acton reported the use of SeO_2 to incorporate the (3*R*) absolute configuration in 3-hydroxyartemisinic acid. The (3*R*) configuration was confirmed through comparison of a known compound from a microbial transformation of artemisinic acid,[17] which resulted in the formation of both (3*R*)- and (3*S*)-hydroxyartemisinic acid and assigned through 2D NOESY experiments that showed a correlation between H-3 and H-10 in the (3*S*)-hydroxyartemisinic acid.[17,18] Nonetheless, we were interested in synthetically accessing the C-3-allylic alcohol derivative to subsequently oxidize and form an enone intermediate. The resulting enone would react with $LiAlD_4$ and $AlCl_3$[19] to potentially yield the dideuterated compound (i.e., Figure 6, **25** to **23**). Initially, dihydroartemisinic acid was treated with $LiAlH_4$ to afford dihydroartemisinic alcohol[20] (Scheme 1, **1** to **26**), which was protected as the *tert*-butyldimethylsilyl (TBDMS) ether **27** (Scheme 1). Subsequent oxidation at the C-3 allylic methylene by refluxing alkene **27** with SeO_2 in EtOH−H_2O (9:1, v/v) resulted in both cleavage of the TBDMS ether and allylic oxidation to afford diol **28**. Diol **28** was crystallized, which allowed for assignment of the (3*R*) absolute configuration (Figure 7A, crystal structure of diol **28**).

Since the TBDMS ether protecting group was labile during the allylic oxidation conditions with SeO_2 (Scheme 1, **27** to **28**), the primary hydroxy group of dihydroartemisinic alcohol was protected as the acetate (Scheme 2, **26** to **29**). The resulting acetate (**29**) was oxidized at C-3 using SeO_2, which kept the 12-acetoxy group intact. The resulting allylic alcohol (**30**) was oxidized with Dess−Martin periodinane to afford enone **31**. Enone **31** was reduced with $AlCl_3$ and $LiAlD_4$ to yield a mixture of the elimination product **32** (Figure 7B, crystal structure of **32**) and 3,3-dideuterodihydroartemisinic alcohol **33**. Alcohol **33** was oxidized with Dess−Martin periodinane to yield 3,3-dideuterodihydroartemisinic aldehyde (**34**). The aldehyde **34** was oxidized under Pinnick oxidation conditions to afford 3,3-dideuterodihydroartemisinic acid (**23**). The ^1H NMR spectra overlay of synthesized 3,3-dideuterodihydroartemisinic acid (**23**) and commercially available dihydroartemisinic acid (**1**) is shown in Figure 8 to confirm the deuterium incorporation at C-3 (boxed δ 1.8−1.9 region).

Use of 3,3-Dideuterodihydroartemisinic Acid (23) to Quantitatively Measure 3,3-Dideuteroartemisinin (24) Formation. In order to measure the formation of 3,3-dideuteroartemisinin (**24**) from 3,3-dideuterodihydroartemisinic acid (**23**), a dried sample of 3,3-dideuterodihydroartemisinic acid (**23**) was left in a vial open to air either in the presence of sunlight (Figure 9) or in complete darkness (Figure 10) (Table 1). Surprisingly, although the amount of d_2-artemisinin (**24**, m/z 285, retention time (t_R) ≈ 3.6 min) was significantly more in the light than in the dark, the amount of d_0-artemisinin (**3**, m/z 283, t_R ≈ 3.6 min) was formed in equal amounts under both conditions (Table 1, entries 1 and 3). This formation of d_0-artemisinin (**3**) was not due to the lack of deuterium incorporation in the synthesized starting material (**23** by LC-HRMS, see Supporting Information), which is confirmed from the fact that the ratio of d_2-artemisinin to d_0-artemisinin (**24** to **3**) is not the same under the light and in the dark conditions (i.e., ∼200:1 with light vs ∼5:1 without light, Table 1, entry 1 vs entry 3). Instead, the formation of d_0-artemisinin (**3**) is likely due to a different mechanism of endoperoxide formation that involves the loss of the deuterium atoms at C-3.

Additionally, monodeuterated artemisinin (Figure 9, **35**) was also detected in the presence of light (Table 1, entry 1, m/z 284.1603). Notably, the use of a high-resolution mass spectrometer was essential in distinguishing ^{13}C-artemisinin and d_1-artemisinin. In other words, the use of an LTQ Orbitrap XL with 100 000 resolving power enabled the resolution of the artemisinin isotopologues with one ^{13}C atom and one deuterium atom ($[M + H]^+$ of m/z 284.1574 and m/z 284.1603), which requires a minimum of 97 986 resolving power ($M/\Delta M$) to distinguish these isotopologues with a 10.2 ppm mass difference.

The fact that the amount of d_0-artemisinin (**3**) was detected at about the same levels both in the light and in the dark (Table 1, entries 1 and 3, areas of 1 860 388 and 1 437 710, respectively) suggests that the conversion of 3,3-d_2-dihydroartemisinic acid to d_0-artemisinin (**23** to **3**) occurs independent of light. Interestingly, because the formation of d_0-artemisinin from 3,3-d_2-dihydroartemisinic acid (**3** from **23**) does not depend on light, its detection could be used to determine the relative rates of conversion of 3,3-d_2-dihydroartemisinic acid to 3,3-d_2-artemisinin (**23** to **24**) with and without light. When no internal standard was added, the ratios of d_2-artemisinin to d_0-artemisinin (**24** to **3**) in the presence and absence of light were 120:1 and 3.4:1 (Figures 9C and 10C), a ∼40-fold difference between d_2-artemisinin and d_0-artemisinin. In addition, the use of d_0-artemisinin as an internal standard allowed for the quantitation of d_2-artemisinin formation both with and without light (cf. Table S1 for calculation of artemisinin formation over time). Using an internal standard, the rates of conversion of 3,3-d_2-dihydroartemisinic acid to 3,3-d_2-artemisinin (**23** to **24**) with and without light were determined to be 1400 ng/day and

Scheme 1. Preliminary Studies Using TBDMS Ether 27 for the Allylic Oxidation with SeO_2 to Give Diol 28

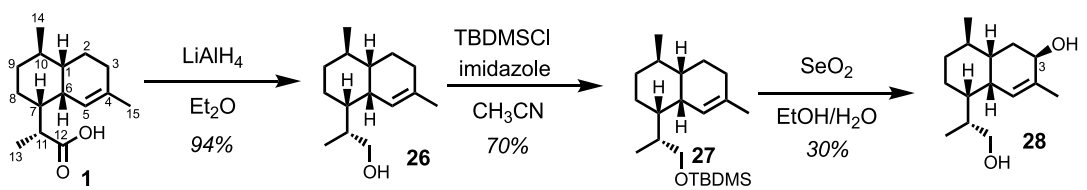

DOI: 10.1021/acs.jnatprod.9b00686
J. Nat. Prod. XXXX, XXX, XXX−XXX

Scheme 2. Synthesis of 3,3-Dideuterodihydroartemisinic Acid (23) from Alcohol 26

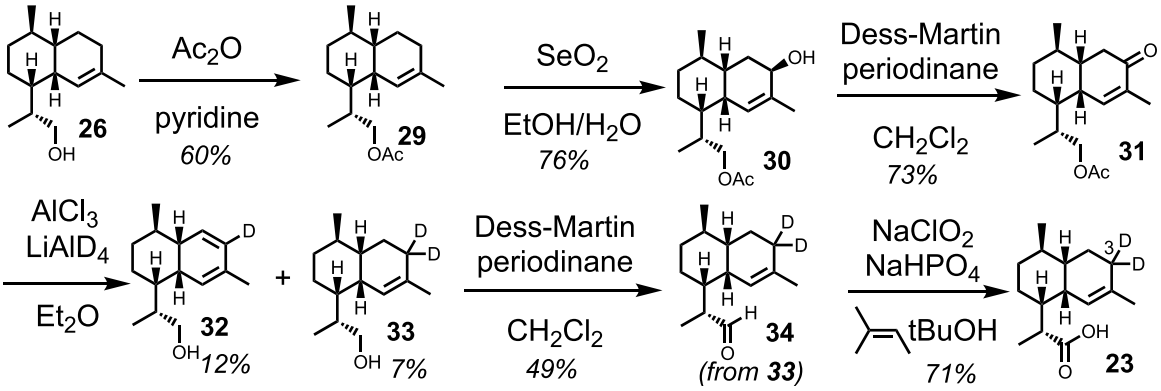

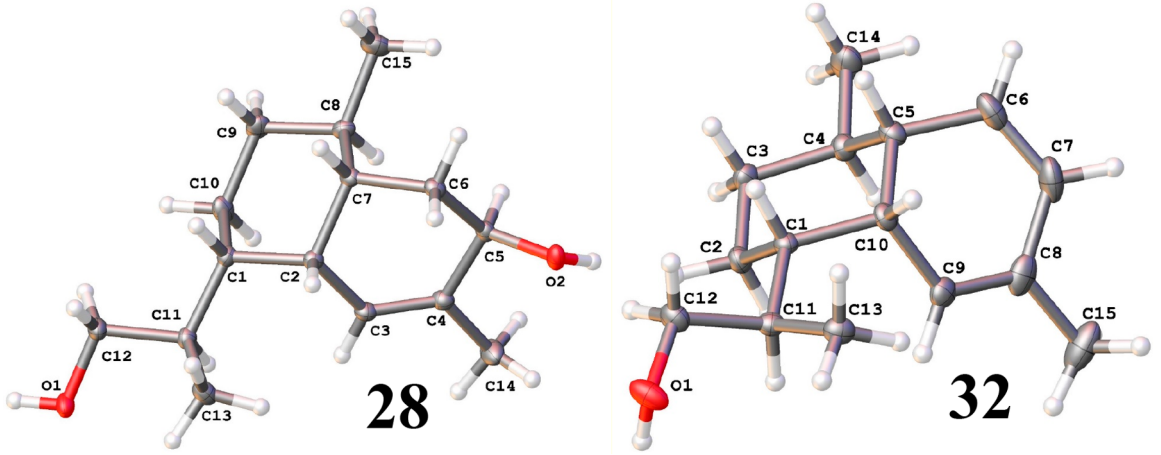

Figure 7. Crystal structures of diol **28** and diene **32**.

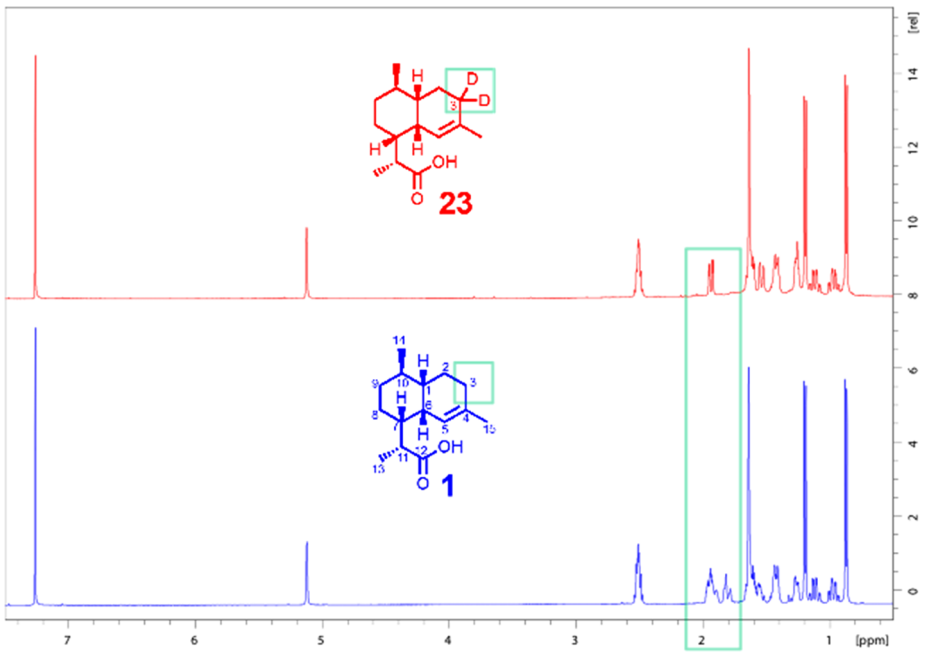

Figure 8. ^{1}H NMR (500 MHz, $CDCl_3$ solvent) spectra overlay of synthesized 3,3-dideuterodihydroartemisinic acid (**23**) and commercially available dihydroartemisinic acid (**1**). Boxed at δ 1.8−1.9 is the C-3 proton region.

32 ng/day (Figures 9B and 10B), also a ∼40-fold difference. The fact that (i) the relative amounts of d_2-artemisinin to d_0-artemisinin (**24** to **3** with light 120 to 1 and without light 3.4 to 1, a 40-fold difference) is the same as (ii) the relative rates of conversion of **23** to **24** with and without light (1400 ng/day and 32 ng/day, also a 40-fold difference) confirms that the

DOI: 10.1021/acs.jnatprod.9b00686
J. Nat. Prod. XXXX, XXX, XXX−XXX

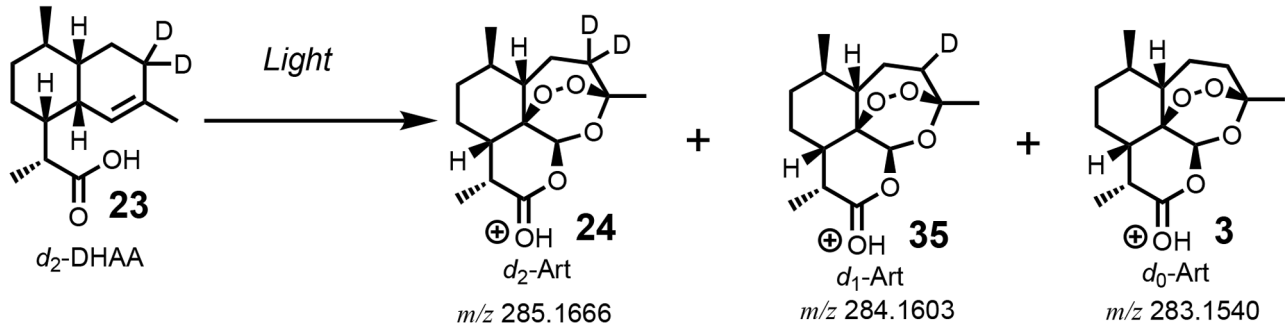

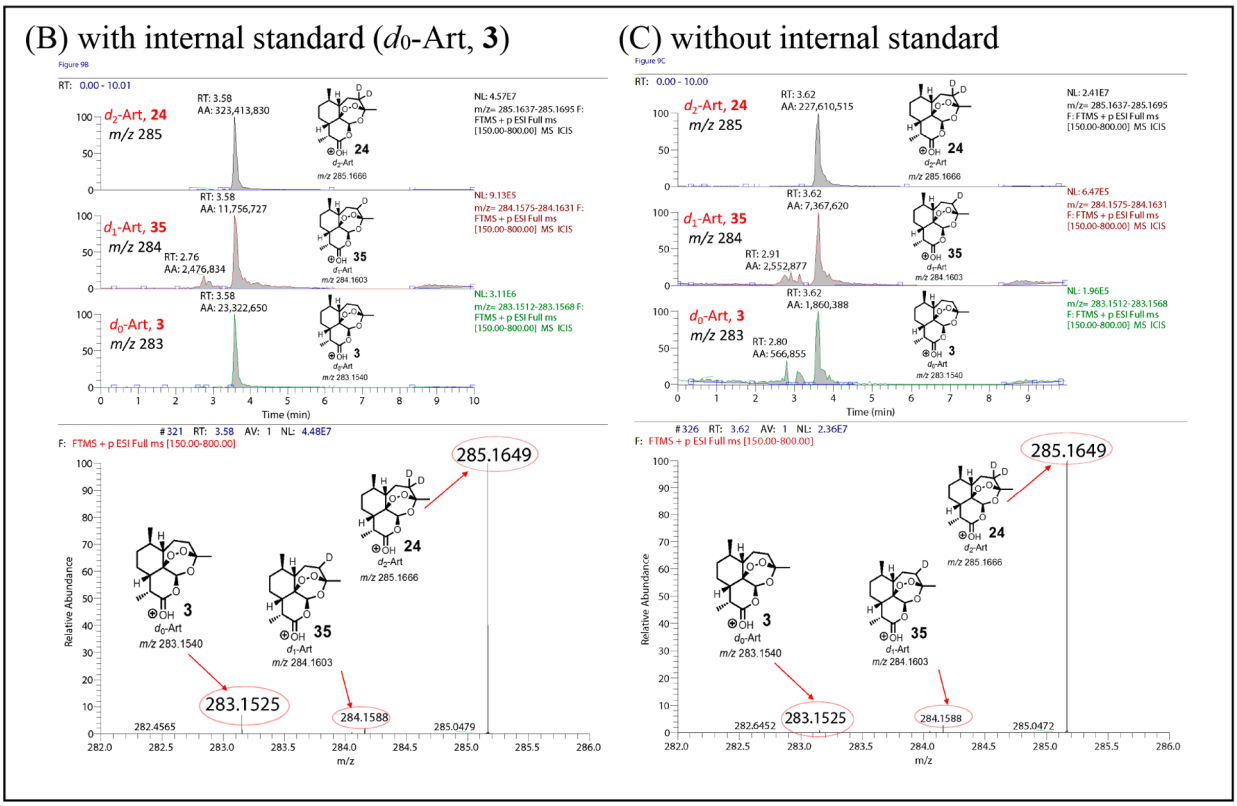

Figure 9. (A) Vials containing d_2-dihydroartemisinic acid (**23**) were exposed to light. The samples were treated under either condition after 13 days: (B) with internal standard (d_0-artemisinin, m/z 283.1540, **3**) or (C) without internal standard (d_0-artemisinin, m/z 283.1540, **3**) and analyzed via LC-HRMS data. Extracted ion chromatogram: d_2-artemisinin (**24**):d_1-artemisinin (**35**):d_0-artemisinin (**3**) (m/z 285.1666, 284.1603, 283.1540). Mass spectrum shown below each chromatogram of peak with retention time (t_R) of ∼3.6 min (range of m/z 282.0−287.1). Electrospray ionization (ESI) positive mode, 10 ppm mass tolerance window.

formation of d_0-artemisinin from d_2-dihydroartemisinic acid (**3** from **23**, both 9 ng/day) is independent of light. These results suggest that the conversion of d_2-dihydroartemisinic acid to d_0-artemisinin (**23** to **3**) occurs at the same rate both with and without light. Importantly, there is likely a kinetic isotope effect at C-3, and this minor mechanistic pathway probably occurs at a faster rate when the C-3 deuterium atoms are not present.[21] Furthermore, a parallel set of time course experiments with another set of vials, the solvent of which was removed with a stream of N_2 gas and immediately capped, were also analyzed for artemisinin production. Other than the caps, these vials, containing 3,3-d_2-dihydroartemisinic acid (**23**), were treated in the same way as the prior experiments shown in Figures 9 and 10. The LC-HRMS data analysis revealed production of artemisinin in these samples presumably due to trace amounts of oxygen in the vial or oxygen permeating through the threads of the cap and the vial (Supporting Information).

The mechanism of conversion of 3,3-d_2-dihydroartemisinic acid to 3,3-d_2-artemisinin (**23** to **24**) is shown in Figure 11. The retention of the two C-3 deuterium atoms is consistent with the mechanisms shown in Figure 2. Moreover, there was also detection of 3-d_1-artemisinin (Figure 9C, m/z 284, **35**), which could be explained by the tautomerization of the methyl ketone intermediate (Figure 11, **13** to **14** to **15**).

DOI: 10.1021/acs.jnatprod.9b00686
J. Nat. Prod. XXXX, XXX, XXX−XXX

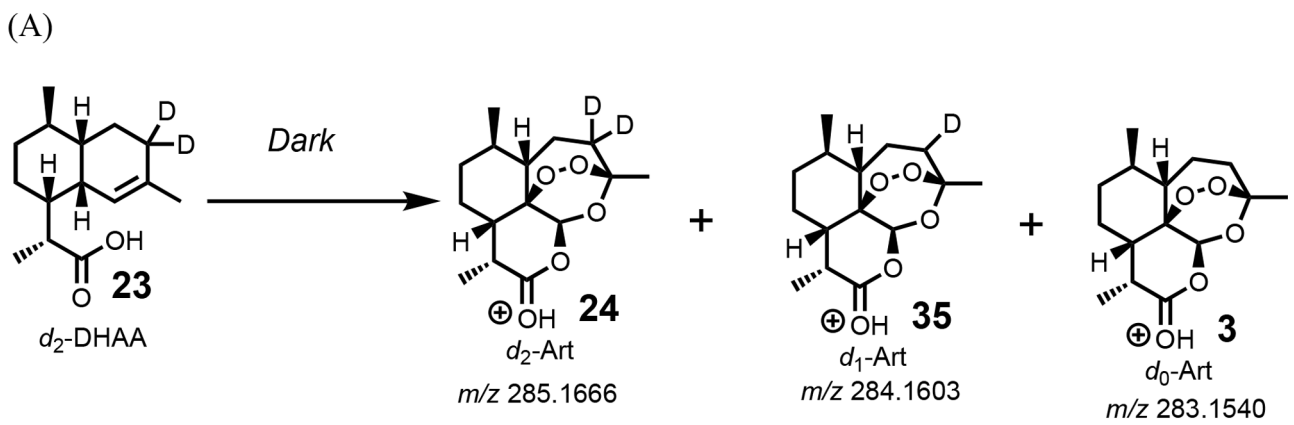

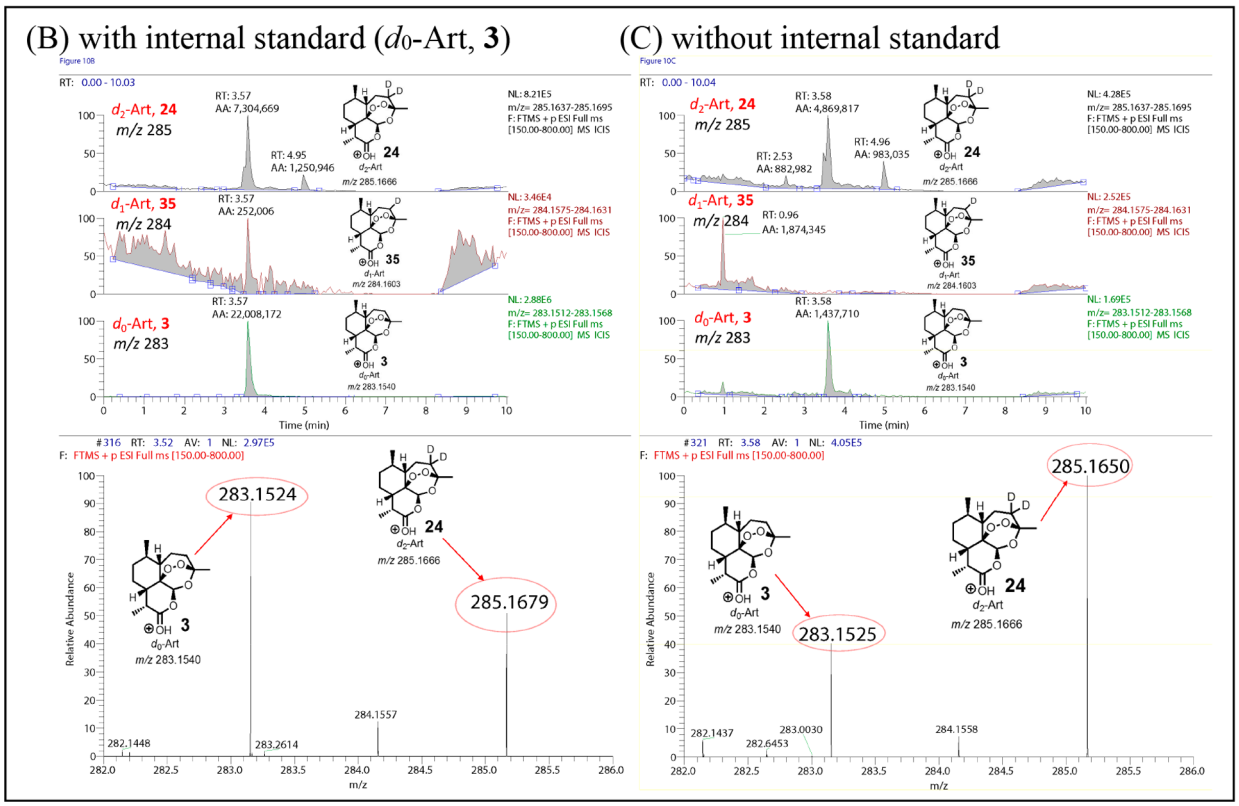

Figure 10. (A) Vials containing d_2-dihydroartemisinic acid (**23**) were kept in darkness, and the samples were treated under the following conditions after 13 days: (B) with internal standard (d_0-artemisinin, m/z 283.1540) and (C) without internal standard (d_0-artemisinin, m/z 283.1540, **3**) and analyzed by LC-HRMS. Extracted ion chromatogram: d_2-artemisinin (**24**):d_1-artemisinin (**35**):d_0-artemisinin (**3**) (m/z 285.1666, 284.1603, 283.1540). Mass spectrum shown below each chromatogram of peak with retention time (t_R) of ~3.6 min (range of m/z 282.0–287.1). Ten ppm mass tolerance window. Electrospray ionization (ESI) positive mode.

The mechanism for the loss of the two C-3 deuterium atoms in the conversion of 3,3-d_2-dihydroartemisinic acid to d_0-artemisinin (**23** to **3**) is proposed through an alkyne intermediate (Figure 11, **42**). Alkyne **42** is formed through the elimination of the C-3 deuterium of dihydro-oxepine **41**, resulting in the regiospecific loss of the two C-3-deuterium atoms (Figure 11). The alkyne intermediate (**42**) is converted to artemisinin as shown in Figure 11b (**42** to **3**). The alkyne intermediate **42** forms the dihydro-oxepine **43** through an endo-dig cyclization. The dihydro-oxepine structure (**43**) has been isolated and reported in an experiment that involved the spontaneous decomposition of dihydroartemisinic acid hydroperoxide (**2**) in $CDCl_3$ in an NMR tube.[6] An alternative endo-dig cyclization from the peroxide intermediate **47** is also shown in Figure 12A to form the endoperoxide **48**, which undergoes cyclization to form artemisinin (**3**). However, this endo-dig cyclization (Figure 11, **42** to **43** or Figure 12A, **47** to **48**) does not have any literature precedence. Therefore, alternative mechanisms for the loss of the two C-3 deuterium atoms are proposed in Figure 12B and C. Figure 12B shows the formation of an alternative allylic hydroperoxide (**50**) from dihydroartemisinic acid (**23**), which undergoes C–C bond

DOI: 10.1021/acs.jnatprod.9b00686
J. Nat. Prod. XXXX, XXX, XXX−XXX

Table 1. LC-HRMS Results for 13-Day Time Point (Data from Figures 9 and 10) Summarized[a]

entry	light	internal std	285.1666 (*m*/*z*)	284.1603 (*m*/*z*)	283.1540 (*m*/*z*)
1	yes	no	227 610 515	7 367 620	1 860 388
2	yes	yes	323 413 830	11 756 727	23 322 650
3	no	no	4 869 817	N.D.	1 437 710
4	no	yes	7 304 669	252 006	22 008 172

[a]Internal standards: 90 μL of a solution of artemisinin (12.7 μg/mL, 2:1 MeOH to CH_2Cl_2, v/v) and 10 μL of a solution of dihydroartemisinic acid (5.7 mg/mL in CH_2Cl_2). Area of peaks corresponding to indicated masses are reported in the table: d_2-artemisinin (**24**) (*m*/*z* 285.1666), d_1-artemisinin (**35**) (*m*/*z* 284.1603), and d_0-artemisinin (**3**) (*m*/*z* 283.1540). N.D.: none detected. Entries 1 and 2: Figure 9B and C, entries 3 and 4: Figure 10B and C.

scission to yield the enolic aldehyde **51**. The resulting enol **51** tautomerizes to lose the deuterium, giving the keto aldehyde **54**, which in turn is converted into artemisinin (**3**). In another mechanistic proposal, as shown in Figure 12C, the monodeuterated dihydro-oxepine **41** (from Figure 11) can form the oxocarbocation **57** through protonation, which can re-form the nondeuterated dihydro-oxepine **43** (Figure 12C). The resulting nondeuterated dihydro-oxepine can undergo endoperoxide formation as shown in Figure 11 (**43** to **3**).

In conclusion, a dried sample of 3,3-dideuterodihydroartemisinic acid (**23**) that was open to air spontaneously converted to 3,3-dideuteroartemisinin (**24**) with and without sunlight at rates of 1400 and 32 ng/day, respectively (~44-fold difference in rate). The formation of artemisinin from dihydroartemisinic acid was detected through ^{1}H NMR spectroscopy to roughly determine the rate of formation of artemisinin from dihydroartemisinic acid (Figure 4). In developing this new technique to quantify the rate of artemisinin formation from dihydroartemisinic acid, a new synthesis of 3,3-dideuterodihydroartemisinic acid (**23**) was developed (Scheme 2). Furthermore, a method using the synthesized 3,3-dideuterodihydroartemisinic acid isotopologue (**23**) and an internal standard of artemisinin (**3**) enabled the quantification of artemisinin production through LC-HRMS (Figure 5). Unexpectedly, nondeuterated artemisinin (**3**) was also formed from the 3,3-dideuterodihydroartemisinic acid (**23**) starting material both with and without light (Figures 9 and 10),

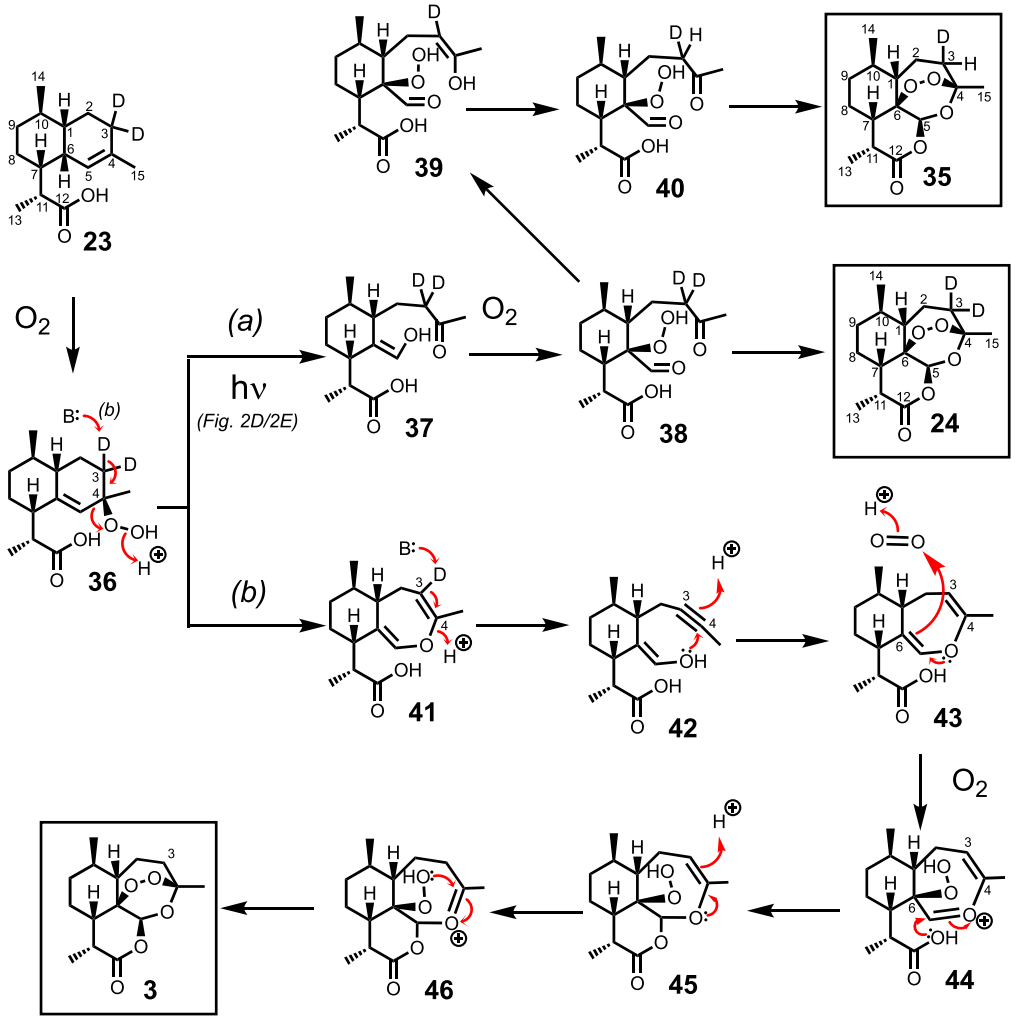

Figure 11. Mechanisms of formation of dideutero-, monodeutero-, and nondeuterated artemisinin isotopologues (**24**, **35**, and **3**) from 3,3-dideuterodihydroartemisinic acid (**23**). Pathway (a) is dominated by the conversion promoted by sunlight to form 3,3-dideuteroartemisinin (**24**). Pathway (b) is the minor pathway that occurs both in the light and in the dark to result in the formation of the loss of the two C-3 deuterium atoms to form nondeuterated artemisinin (**3**).

DOI: 10.1021/acs.jnatprod.9b00686
J. Nat. Prod. XXXX, XXX, XXX−XXX

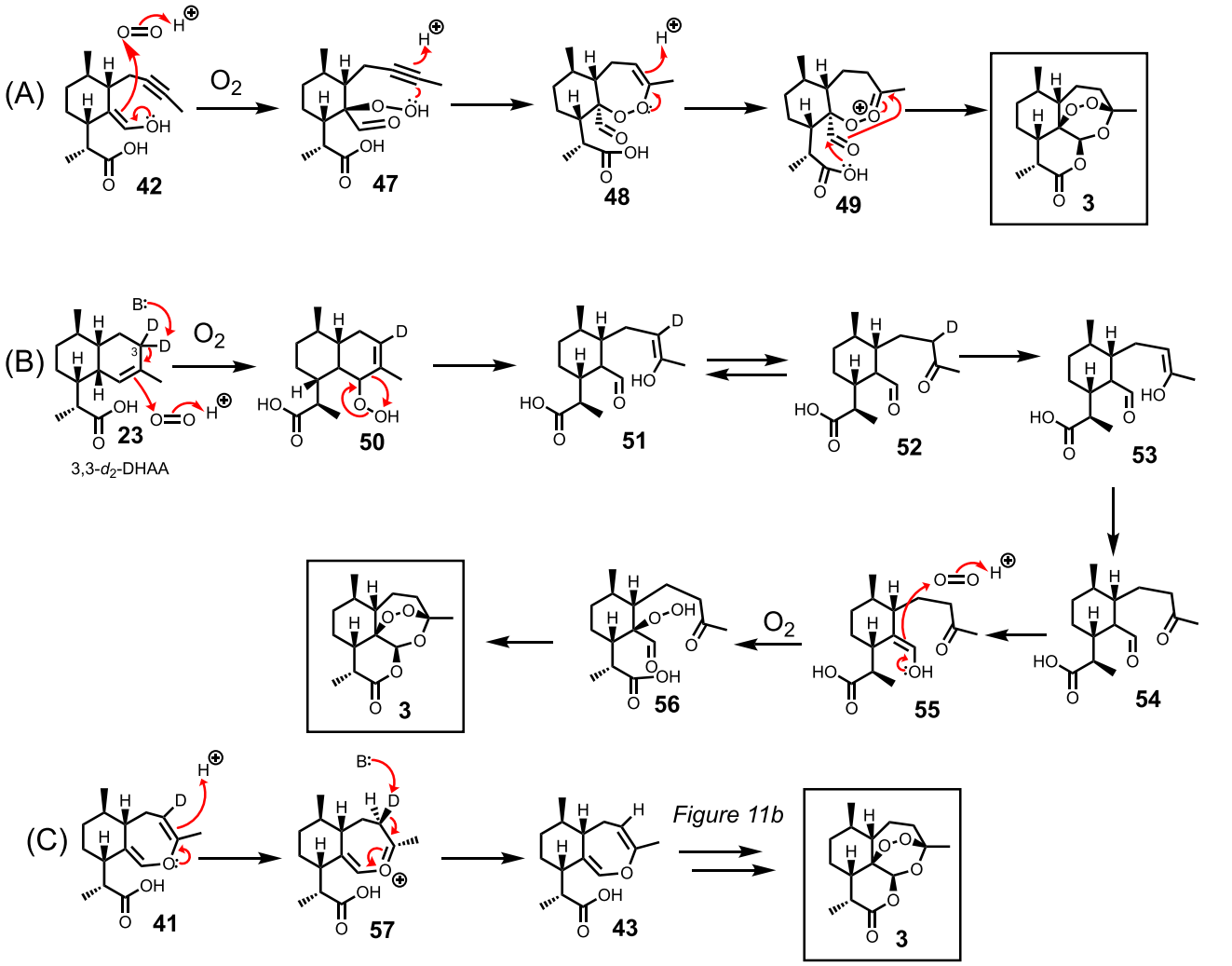

Figure 12. Alternative pathways (vs Figure 11b) leading to the formation of nondeuterated artemisinin (**3**) from (A) alkyne intermediate **42**, (B) 3,3-d_2-dihydroartemisinic acid **23**, and (C) dihydro-oxepine **41**.

suggesting that a minor mechanistic pathway is operative to form the endoperoxide ring of artemisinin, which involves the loss of the two C-3 deuterium atoms. This minor pathway likely occurs at a faster rate when there are no C-3 deuterium atoms present in dihydroartemisinic acid due to a kinetic isotope effect (i.e., stronger C−D bond vs weaker C−H bond). In the presence of sunlight, the formation of the endoperoxide from 3,3-dideuterodihydroartemisinic acid (**23**) retains the two C-3 deuterium atoms to yield 3,3-d_2-artemisinin (**24**) (Figure 9). Although an enzymatic conversion of dihydroartemisinic acid to artemisinin is not ruled out, the mechanisms proposed for this nonenzymatic transformation of dihydroartemisinic acid to artemisinin may reflect how the endoperoxide of artemisinin is formed in nature.

EXPERIMENTAL SECTION

General Experimental Procedures. Melting points were recorded on a melting point apparatus (Global Medical and Lab Solutions, India, or Optimelt MPA100/Stanford Research Systems, Sunnyvale, CA, USA). Optical rotations were recorded on an Autopol IV polarimeter (Rudolph Research, Hackettstown, NJ, USA). IR data were acquired on an FTIR system (Nicolet iS50 FT-IR spectrometer, Thermo Fisher Scientific, Waltham, MA, USA). IR data were analyzed on OMNIC software (Thermo Fisher Scientific). NMR spectra were recorded on a Bruker 500 MHz spectrometer (Bruker, Billerica, MA, USA). NMR data were analyzed on Topspin software (Bruker). HRMS data were acquired on an LTQ Orbitrap XL instrument (Thermo Fisher Scientific) connected to a Waters Acquity UPLC system (Waters Corp, Milford, MA, USA). MS data were analyzed on Qualbrowser software (Thermo Fisher Scientific). The UPLC column used was a Phenomenex (Torrance, CA, USA), Synergi 4 μm, Fusion-RP (reverse-phase) 80 Å. TLC plates with 254 nm fluorescent indicator were used.

LC-MS Conditions. Samples were run on an Acuity UPLC connected to an LTQ Orbitrap XL mass spectrometer. The liquid chromatography conditions were set as follows: mobile phase A was 0.01% formic acid in water, v/v, and mobile phase B was 0.01% formic acid in MeCN, v/v. The flow rate was 0.6 mL/min. The gradient was as follows (over 10 min): from 0 to 1 min, 98% mobile phase A; 1 to 3 min, the gradient shifted from 98% A to 50% A; 3 to 6 min, 50% A to 2% A; from 6 to 7.9 min held at 2% A; 7.9 to 8 min, from 2% A to 98% A; 8 to 10 min, 98% A. The mass spectrometer was tuned with a solution of 1 mM artemisinin in MeOH. The tuning conditions were as follows: sheath gas flow rate 35, aux gas flow rate 8, sweep gas flow rate 0, spray voltage (kV) 5.00, capillary temperature 250 °C, capillary voltage 14 V, tube lens 125 V. Before mass spectrometry samples were run on the instrument, the mass spectrometer was calibrated using a Pierce LTQ ESI positive calibration ion solution (Thermo Fisher, catalog number: 88322); see Supporting Information for calibration results. Each injection was 10 μL of volume for data shown in Figures 9 and 10. Samples were analyzed under electrospray ionization positive mode (ESI-positive mode).

DOI: 10.1021/acs.jnatprod.9b00686
J. Nat. Prod. XXXX, XXX, XXX−XXX

Time Course of Dihydroartemisinic Acid to Artemisinin (1 to 3) Monitored by ^{1}H NMR Spectroscopy. A solution of dihydroartemisinic acid (**1**) in CH_2Cl_2 (1.0 g in 50 mL) was divided into 40 clear glass vials and 40 amber glass vials at 0.5 mL per vial. After drying the solution first with a stream of N_2 and then under house vacuum in a desiccator, the clear glass vials were let to stand by the window sill open to air while the amber glass vials were placed in a black box in a cabinet in total darkness. Various time points were taken by dissolving the dried samples in $CDCl_3$ (0.7 mL) to monitor the formation of artemisinin (**3**).

Time Course of 3,3-d_2-Dihydroartemisinic Acid (23) to Artemisinin (3, 24, and 35) Monitored by HRMS. A solution of 3,3-d_2-dihydroartemisinic acid (**23**) (2.7 mg) in CH_2Cl_2 (2 mL) was aliquoted into 20 2 mL clear glass vials and 20 2 mL amber glass vials with the addition of 50 μL for each vial. The solvent was evaporated under house vacuum in a desiccator. The clear glass vials containing **23** were placed in a clear plastic vial rack on the window sill. The amber glass vials with **23** were placed in a black plastic box, which was stored in a cabinet. At different time points, the compounds were extracted through two different methods: [i] with internal standards (e.g., Figure 9B) and [ii] without internal standards (e.g., Figure 9C). The solvents in four vials in each set were blown down with a stream of N_2 and quickly sealed with a cap (Supporting Information for LC-MS traces).

[i] With internal standards: 90 μL of solution B and 10 μL of solution D were added. Solution B was 12.7 μg of artemisinin in 1 mL of a MeOH–CH_2Cl_2 (2:1, v/v) mixture, and solution D was 5.65 mg of dihydroartemisinic acid in 1 mL of CH_2Cl_2.

[ii] Without internal standards: 100 μL of MeOH was added. When analyzing for d_0-artemisinin (**3**), d_1-artemisinin (**35**), and d_2-artemisinin (**24**), the following masses were searched for through extracted ion chromatography: m/z 283.1540, 284.1603, and 285.1666 with a 10 ppm mass tolerance window. The mass for ^{13}C-labeled artemisinin was m/z 284.1574.

Synthesis of 2*R*-(1*R*,4*R*,4a*S*,8a*S*)-4,7-Dimethyl-1,2,3,4,4a,5,6,8a-octahydronaphthalen-1-yl)propan-1-ol (26). Dihydroartemisinic acid (**1**, 30.0 g, 127 mmol) in Et_2O (150 mL) was added to a suspension of $LiAlH_4$ (19.3 g, 508 mmol, 4 molar equiv) in Et_2O (100 mL) at −78 °C under an atmosphere of N_2. The reaction was stirred for 30 min, warmed to room temperature, and left stirring for 3 h at room temperature. The reaction mixture was cooled to −78 °C, and acetone (100 mL) was added dropwise, followed by Rochelle's salt (30 g, 110 mmol) in water (100 mL) (added dropwise) by an addition funnel at −78 °C. The reaction mixture was filtered using a fritted filter funnel to afford dihydroartemisinic alcohol (**26**) as a white solid (28.2 g, 128 mmol, 94%). No further purification was done; R_f 0.56 (hexanes–EtOAc, 4:1, v/v); $[\alpha]^{20}_D$ +10.2 [c 5.6 mg/mL in $CHCl_3$]; IR (neat) 3401.44, 3328.95, 2962.73, 2919.27, 2864.28, 2842.95 cm^{-1}; ^{1}H NMR (500 MHz, $CDCl_3$) δ 5.21 (s, 1 H), 3.74 (dd, J_1 = 14 Hz, J_2 = 7.4 Hz, 1H), 3.52 (dd, J_1 = 16.8 Hz, J_1 = 4.3 Hz, 1H), 2.47 (s, 2H), 1.65–1.50 (m, 6H), 1.63 (br s, 3H), 0.99 (m, 4H); ^{13}C NMR (125 MHz, $CDCl_3$) δ 135.1, 120.6, 66.73, 42.62, 42.01, 41.73, 37.44, 36.58, 36.36, 35.59, 27.62, 26.62, 26.29, 25.77, 23.77, 19.73, 14.92; HRMS (m/z) calculated for $C_{15}H_{27}O$ [M + H]$^+$, 223.2056; found, 223.2039 (Δ 7.62 ppm); mp 72.3–72.8 °C.

Synthesis of (*R*)-2-((1*R*,4*R*,4a*S*,8a*S*)-1,2,3,4,4a,5,6,8a-Octahydro-4,7-dimethylnaphthalen-1-yl)propyl *tert*-Butyldimethylsilyl Ether (27). Imidazole (5.0 g, 73.4 mmol, 4.7 molar equiv) and TBDMSCl (3.1 g, 20.6 mmol, 1.3 molar equiv) were added to a solution of alcohol **26** (3.5 g, 15.8 mmol) in MeCN (200 mL). After the reaction mixture was stirred for 1 h, EtOAc (500 mL) was added, and the reaction mixture was diluted with water (200 mL). The organic layer was concentrated under reduced pressure to afford TBDMS ether **27** as a clear oil (3.7 g, 11 mmol, 70%): R_f 0.61 (100% hexanes); $[\alpha]^{20}_D$ −30.0 [c 1.0 mg/mL in $CHCl_3$]; IR (neat) 2953.45, 2925.01, 2905.90, 2854.10, 1707.34 cm^{-1}; ^{1}H NMR (500 MHz, $CDCl_3$) δ 5.22 (br s, 1 H), 3.68 (dd, J_1 = 9.7 Hz, J_2 = 3.2 Hz, 1H), 3.41 (dd, J_1 = 9.7 Hz, J_2 = 4.5 Hz, 1H), 2.49–2.43 (m, 1H), 1.96–1.85 (m, 2H), 1.84–1.75 (m, 1H), 1.65–1.51 (m, 4H), 1.63 (br s, 3H), 1.47–1.37 (m, 1H), 1.22–1.13 (m, 2H), 0.94 (d, J = 6.4 Hz, 3H), 0.91 (s, 3H), 0.90 (s, 9H), 0.86 (d, 6.7 Hz, 3H), 0.03 (br s, 6H); ^{13}C NMR (125 MHz, $CDCl_3$) δ 135.0, 121.3, 67.0, 42.9, 42.3, 37.7, 36.9, 35.9, 27.9, 26.9, 26.6, 25.8, 24.0, 20.0, 18.5, 15.4, −3.43, −5.26. HRMS run on ESI positive mode, but ion not found due to small molecule not ionizing.

Synthesis of (*R*)-2-((1*R*,4*R*,4a*S*,6*R*,8a*S*)-1,2,3,4,4a,5,6,8a-Octahydro-6-hydroxy-4,7-dimethylnaphthalen-1-yl)propan-1-ol (28). SeO_2 (0.31 g, 2.8 mmol, 1 molar equiv) was added to a solution of TBDMS ether **27** (0.93 g, 2.8 mmol) in a mixture of EtOH and water (30 mL, 9:1, v/v). The reaction mixture was heated under reflux for 6 h. The reaction mixture was diluted with EtOAc (200 mL) and washed with water (2 × 50 mL). The organic layer was concentrated by reduced pressure and purified by column chromatography (silica gel, 100% hexanes to 10% hexanes in EtOAc, v/v) to yield diol **28** as a solid (0.20 g, 0.84 mmol, 30%). The solid was dissolved in EtOAc and hexanes (3 mL, 1:1 EtOAc and hexanes, v/v) and left in the hood for 2 days to afford block-shaped crystals. R_f 0.42 (hexanes–EtOAc, 1:1, v/v); $[\alpha]^{20}_D$ +7.0 [c 3.4 mg/mL in $CHCl_3$]; IR (neat) 3373.02, 3315.64, 2924.65, 2865.61, 1705.31, 1661.08 cm^{-1}; ^{1}H NMR (500 MHz, $CDCl_3$) δ 5.35 (br s, 1H), 4.14–4.07 (m, 1H), 3.74 (dd, J_1 = 10 Hz, J_2 = 3.1 Hz, 1H), 3.53 (dd, J_1 = 10.4 Hz, J_2 = 6.0 Hz, 1H), 2.59–2.54 (m, 1H), 2.40 (ddd, J_1 = 12 Hz, J_2 = 5.7 Hz, 1H, J_3 = 2.4 Hz, 1H), 1.76 (br s, 3H), 1.75–1.55 (m, 4H), 1.51–1.34 (m, 4H), 1.25–1.16 (m, 2H), 1.00 (d, J = 6.8 Hz, 1H), 0.91 (d, J = 5.7 Hz, 1H); ^{13}C NMR (125 MHz, $CDCl_3$) δ 136.9, 124.6, 68.9, 66.8, 44.9, 42.6, 38.2, 37.06, 36.95, 35.7, 29.0, 26.6, 19.9, 19.8, 15.1; HRMS (m/z) calculated for $C_{15}H_{27}O_2$ [M + H]$^+$, 239.2006; found, 239.1987 (Δ 7.94); mp 107.2–107.5 °C.

Synthesis of (*R*)-2-((1*R*,4*R*,4a*S*,8a*S*)-1,2,3,4,4a,5,6,8a-Octahydro-4,7-dimethylnaphthalen-1-yl)propyl Acetate (29). Ac_2O (14 mL, 150 mmol, 2.0 molar equiv) was added to a solution of alcohol **26** (16.0 g, 72.3 mmol, 1 molar equiv) in pyridine (100 mL, 0.7 M). The reaction mixture was stirred for 30 min, and the resulting solution diluted with water and extracted with Et_2O (3 × 100 mL). The organic layer was concentrated under reduced pressure, and the resulting oil was filtered through a short pad of silica gel with 200 mL of 50/50 EtOAc–hexanes, v/v, to afford acetate **29** as a colorless oil (11.5 g, 43.5 mmol, 60%): R_f 0.76 (hexanes–EtOAc, 4:1, v/v); $[\alpha]^{20}_D$ −72.2 [c 2.3 mg/mL in $CHCl_3$]; IR (neat) 2959.61, 2908.35, 2867.57, 2851.13, 1738.20 cm^{-1}; ^{1}H NMR (500 MHz, $CDCl_3$) δ 5.18 (s, 1H), 4.19 (dd, J_1 = 11 Hz, J_2 = 3.2 Hz, 1H), 3.89 (dd, J_1 = 11 Hz, J_2 = 6.9 Hz, 1H), 22.48 (s, 1H), 2.05 (s, 3H), 1.95 (m, 1H), 1.94–1.91 (m, 2H), 1.83- 1.77 (m, 2H), 1.63 (br s, 3H), 1.59–1.52 (m, 2H), 1.50–1.35 (m, 1H), 1.26–1.17 (m, 3H), 1.07–0.98 (m, 1 H), 0.97 (d, J = 7.1 Hz, 3H), 0.91 (d, J = 3.0 Hz, 1H), 0.86 (d, J = 6.9 Hz, 3H); ^{13}C NMR (125 MHz, $CDCl_3$) δ 171.5, 135.5, 120.5, 68.70, 43.32, 42.15, 37.55, 35.70, 33.97, 27.78, 26.79, 26.44, 25.94, 23.94, 21.12, 19.89, 15.46; HRMS (m/z) calculated for $C_{17}H_{29}O_2$ [M + H]$^+$, 265.2162; found, 265.2138 (Δ 9.05 ppm).

Synthesis of (*R*)-2-((1*R*,4*R*,4a*S*,6*R*,8a*S*)-1,2,3,4,4a,5,6,8a-Octahydro-6-hydroxy-4,7-dimethylnaphthalen-1-yl)propyl Acetate (30). SeO_2 (12.65 g, 114.0 mmol, 1 molar equiv) was added to a solution of EtOH (200 mL), water (20 mL), and acetate **29** (30.0 g, 114.0 mmol, 1 molar equiv). The reaction mixture was refluxed at 90 °C for 10 h, cooled to rt, and diluted with EtOAc (200 mL). The resulting solution was washed with water (200 mL), and the organic layer was concentrated by reduced pressure. The crude material was purified by silica gel column chromatography (90% hexanes in EtOAc, v/v, to 10% hexanes in ethyl acetate, v/v) to afford allylic alcohol **30** as a yellow oil (22.85 g, 81.5 mmol, 76%): R_f 0.38 (hexanes–EtOAc, 4:1, v/v); $[\alpha]^{20}_D$ +31.1 [c 5.1 mg/mL in $CHCl_3$]; IR (neat) 3390.21, 2910.02, 2867.15, 2850.37, 1736.83, 1722.03 cm^{-1}; ^{1}H NMR (500 MHz, $CDCl_3$) δ 5.33 (s, 1H), 4.18 (dd, J_1 = 11 Hz, J_2 = 3.4 Hz, 1H), 4.13–4.07 (m, 1H), 3.90 (dd, J_1 = 11 Hz, J_2 = 7.0 Hz, 1H), 2. 57 (s, 1H), 2.06 (s, 3H), 1.80–1.75 (m, 1H), 1.76 (br s, 3H), 1.56 (s, 1H), 1.50–1.45 (m, 1H), 1.38 (s, 2H), 1.20–1.14 (m, 2H), 1.02- 0.97 (m, 2H), 0.97 (d, J = 6.9 Hz, 3H), 0.91 (d, J = 6.1 Hz, 3H); ^{13}C NMR (125 MHz, $CDCl_3$) δ 171.5, 137.1, 124.3, 68.83, 68.51, 44.82, 43.15, 38.04, 36.99, 35.60, 34.16, 28.93, 26.49, 21.14, 19.83, 19.77, 15.45;

DOI: 10.1021/acs.jnatprod.9b00686
J. Nat. Prod. XXXX, XXX, XXX–XXX

HRMS (*m/z*) calculated for $C_{17}H_{29}O_3$ $[M + H]^+$, 281.2111; found, 281.2085 (Δ 9.25 ppm).

Synthesis of (*R*)-2-((1*R*,4*R*,4a*S*,8a*S*)-1,2,3,4,4a,5,6,8a-Octahydro-6-keto-4,7-dimethylnaphthalen-1-yl)propyl Acetate (31). Dess–Martin periodinane (19.45 g, 45.9 mmol, 1 molar equiv) was added to a solution of allylic alcohol **30** (12.85 g, 45.9 mmol) in CH_2Cl_2 (250 mL). The resulting solution was diluted with CH_2Cl_2 (100 mL) and washed with saturated $Na_2S_2O_4$ (aqueous, 100 mL). The organic layer was washed with saturated $NaHCO_3$ (aqueous, 100 mL). The organic layer was concentrated under reduced pressure and purified by silica gel chromatography (90% CH_2Cl_2 to 10% EtOAc). The crude residue was washed with water and $NaHCO_3$ and concentrated under reduced pressure to obtain enone **31** as a yellow solid (9.4 g, 33.8 mmol, 73%): R_f 0.51 (hexanes–EtOAc, 4:1, v/v); $[\alpha]^{20}_D$ +92.5 [*c* 5.4 mg/mL in $CHCl_3$]; IR (neat) 2955.34, 2941.67, 2920.93, 2905.21, 2878.09, 2851.31, 1731.93, 1666.76 cm^{-1}; ^1H NMR (500 MHz, $CDCl_3$) δ 6.49 (s, 1H), 4.22 (dd, J_1 = 11 Hz, J_2 = 3.4 Hz, 1H), 3.95 (dd, J_1 = 11 Hz, J_2 = 6.8 Hz, 1H), 2.91 (br s, 1H), 2.75 (dd, J_1 = 17 Hz, J_2 = 2.6 Hz,, 1H), 2.44 (dd, J_1 = 17 Hz, J_2 = 4.9 Hz, 1H), 2.07 (s, 3H), 1.85–1.82 (m, 1H), 1.77 (br s, 3H), 1.49–1.44 (m, 1H), 1.36–1.30 (m, 1H), 1.05 (m, 3H), 1.01 (d, *J* = 7.2 Hz, 1H), 0.97–0.92 (m, 1H), 0.85 (d, *J* = 6.2 Hz, 1H); ^{13}C NMR (125 MHz, $CDCl_3$) δ 199.9, 171.4, 144.1, 136.9, 68.08, 46.14, 43.08, 39.31, 35.33, 34.24, 28.79, 26.96, 21.11, 19.65, 16.21, 15.55; HRMS (*m/z*) calculated for $C_{17}H_{27}O_3$ $[M + H]^+$, 279.1955; found, 279.1929 (Δ 9.31 ppm); mp 98.0–99.4 °C.

*To remove an aldehyde impurity (see Supporting Information), which coeluted with the enone product (**9**) derived from the formation of the primary allylic alcohol in the SeO_2 oxidation, the purified enone was subjected to Pinnick oxidation conditions to convert the aldehyde impurities to corresponding carboxylic acids, which would be removed upon basic aqueous workup: A solution of NaH_2PO_4 (4.15 g, 34.61 mmol, 0.83 molar equiv) in water (25 mL) and NaOCl (3.77 g, 20.9 mmol, 0.5 molar equiv) were added to a solution of enone **31** (9.69 g, 41.7 mmol) in *t*-BuOH (4.38 mL) and 2-methyl-2-butene (5.43 mL). The mixture was washed with $NaHCO_3$ (saturated aqueous solution, 100 mL) and extracted with EtOAc (3 × 50 mL). The organic layer was concentrated by reduced pressure. The crude material was purified by silica gel column chromatography (90% hexanes in EtOAc, v/v, to 10% hexanes in EtOAc, v/v) to yield pure enone **31** (7.1 g, 30.6 mmol, 73%) as a white solid (see Supporting Information for structures).

Synthesis of (*R*)-2-((1*R*,4*R*,4a*S*,8a*S*)-6,6-Dideutero-1,2,3,4,4a,5,6,8a-octahydro-4,7-dimethylnaphthalen-1-yl)-propan-1-ol (33). $LiAlD_4$ (0.68 g, 16.19 mmol, 4.5 molar equiv) was added to a solution of $AlCl_3$ (8.63 g, 64.7 mmol, 18 molar equiv) in Et_2O (100 mL) at −78 °C. The reaction flask was evacuated and backfilled with N_2. After 5 min, enone **31** (1.00 g, 3.59 mmol, 1.5 molar equiv) dissolved in Et_2O (100 mL) was added. The reaction mixture was gradually warmed to room temperature and stirred for an additional 10 h. The mixture was cooled to −78 °C and quenched with water (100 mL). The resulting solution was diluted with EtOAc (200 mL). The organic layer was concentrated under reduced pressure. The crude material was purified by silica gel column chromatography (100% hexanes to 10% EtOAc in hexanes, v/v, to 20% EtOAc in hexanes, v/v) to afford a mixture of alcohol (**33**) and diene **32** as a white solid. Diene **32** was slightly more polar than monoalkene **33** (i.e., when the compounds eluted off of the column, the mixture was collected in 10 test tubes (20 mL volume each tube), and the solvent in each tube was evaporated; the resulting compound was characterized by ^1H NMR spectroscopy). The mixture of **33** (59 mg, 0.26 mmol, 7%) and **32** (98 mg, 0.44 mmol, 12%) was further separated through a second column. *All compound characterization is for monoalkene (**33**): R_f 0.49 (hexanes–EtOAc, 4:1, v/v); $[\alpha]^{20}_D$ −54.6 [*c* 1.7 mg/mL in $CHCl_3$]; IR (neat) 3398.21, 3328.32, 2962.93, 2919.63, 2863.37, 2842.91, 2160.84, 2127.28, 2082.21, 2023.07, 1716.14, 1661.06, 1558.32 cm^{-1}; ^1H NMR (500 MHz, $CDCl_3$) δ 5.21 (s, 1H), 3.74 (dd, J_1 = 11 Hz, J_2 = 2.7 Hz, 1H), 3.52 (m, 1H), 2.47 (s, 1H), 1.91 (dd, J_1 = 14 Hz, J_2 = 3.6 Hz,, 1H), 1.62 (br s, 3H), 1.56–1.49 (m, 1H), 1.48–1.36 (m, 1H), 1.25–1.18 (m, 3H), 0.99 (d, J = 6.8 Hz, 3H), 0.97- 0.89 (m, 2H), 0.86 (d, *J* = 6.8 Hz, 3H); ^{13}C NMR (125 MHz, $CDCl_3$) δ 135.3, 120.9, 66.97, 42.84, 42.23, 37.68, 36.81, 35.82, 27.85, 26.51, 25.80, 23.97, 19.96, 15.14, 1.16; HRMS (*m/z*) calculated for $C_{15}H_{25}D_2O$ $[M + H]^+$, 225.2182; found, 225.2160 (Δ9.77 ppm); mp 64.5–65.5 °C. *This reaction is water sensitive, and oven-dried glassware, dried under N_2 atmosphere, were used. Although the diene **32** was visible on the TLC plate under a UV lamp, the R_f values of the monoalkene **33** and diene **32** were identical by TLC. When the reaction conditions were not dry (i.e., water condensed during the reaction), the reaction mixture turned pink in color, and the major product was diene **32**.

Synthesis of (*R*)-2-((1*R*,4*R*,4a*S*,8a*S*)-6,6-Dideutero-1,2,3,4,4a,5,6,8a-octahydro-4,7-dimethylnaphthalen-1-yl)-propan-1-al (34). Dess–Martin periodinane (52.0 mg, 0.12 mmol, 1.1 molar equiv) was added to a solution of alcohol **33** (24.0 mg, 0.11 mmol, 1 molar equiv) in CH_2Cl_2 (50 mL) at room temperature. The reaction mixture was stirred for 1 h, directly loaded on a column packed with a slurry of silica gel in hexanes, and purified by column chromatography (100% hexanes to 50% EtOAc in hexanes, v/v) to afford aldehyde **33** as a white solid (12 mg, 0.05 mmol, 49%): R_f 0.58 (hexanes–EtOAc, 4:1, v/v); $[\alpha]^{20}_D$ +221.1 [*c* 2.0 mg/mL in $CHCl_3$]; IR (neat) 3393.83, 2922.14, 2868.88, 1704.93 cm^{-1}; ^1H NMR (500 MHz, $CDCl_3$) δ 9.58 (d, *J* = 4.02, 1H), 5.12 (s, 1H), 2.48 (s, 1H), 2.39 (m, 1 H), 1.94 (dd, J_1 = 13 Hz, J_2 = 3.2 Hz, 1H), 1.64 (br s, 3H), 1.54 (d, J = 12.6 Hz, 2H), 1.48–1.39 (m, 3H), 1.29–1.25 (m, 2H), 1.15–1.09 (m, 2H), 1.07 (d, *J* = 6.8 Hz, 4H), 1.02–0.91 (m, 2H), 0.88 (d, *J* = 6.3 Hz, 4H); ^{13}C NMR (125 MHz, $CDCl_3$) δ 206.2, 134.5, 119.8, 48.59, 41.99, 41.63, 36.75, 35.41, 27.86, 27.49, 25.70, 23.94, 19.84, 11.90; HRMS (*m/z*) calculated for $C_{15}H_{23}D_2O$ $[M + H]^+$, 223.2025; found, 223.2004 (Δ9.40 ppm); mp 124.5–127.3 °C.

Synthesis of (*R*)-2-((1*R*,4*R*,4a*S*,8a*S*)-6,6-Dideutero-1,2,3,4,4a,5,6,8a-octahydro-4,7-dimethylnaphthalen-1-yl)-propan-1-oic acid (23). A solution of NaH_2PO_4 (65.9 mg, 0.55 mmol, 10 molar equiv) in water (2 mL) and NaOCl (29.8 mg, 0.33 mmol, 6 molar equiv) were added to a solution of aldehyde **33** (12.7 mg, 0.06 mmol, 1 molar equiv) in *t*-BuOH (5.71 mL) and 2-methyl-2-butene (0.54 mL). The reaction mixture was extracted with EtOAc (3 × 50 mL), and the organic layer concentrated under reduced pressure to afford carboxylic acid **23** as a white solid (9.0 mg, 0.04 mmol, 71%). No further purification was done. R_f 0.85 (hexanes–EtOAc, 4:1, v/v); $[\alpha]^{20}_D$ −15.0 [*c* 1.1 mg/mL in $CHCl_3$]; IR (neat) 2961.19, 2920.51, 2867.51, 2851.48, 1704.76 cm^{-1}; ^1H NMR (500 MHz, $CDCl_3$) δ 5.12 (s, 1H), 3.36 (s, 1H), 1.93 (dd, J_1 = 14 Hz, J_2 = 3.5 Hz, 1H), 1.67–1.58 (m, 2H), 1.66 (br s, 3H), 1.54 (dd, J_1 = 14 Hz, J_2 = 2.0 Hz, 1H), 1.48–1.38 (m, 2H), 1.29–1.23 (m, 2H), 1.19 (d, *J* = 6.9 Hz, 3H), 1.12 (qd, J_1 = 13 Hz, J_2 = 3.3 Hz, 1H), 0.97 (qd, J_1 = 13 Hz, J_2 = 3.3 Hz, 1H), 0.87 (d, *J* = 6.3 Hz, 3H); ^{13}C NMR (125 MHz, $CDCl_3$) δ 181.0, 136.1, 119.5, 43.81, 41.96, 41.86, 36.51, 35.39, 29.85, 27.83, 27.58, 25.72, 23.95, 19.85, 15.27; HRMS (*m/z*) calculated for $C_{15}H_{23}D_2O_2$ $[M + H]^+$, 239.1975; found, 239.1971 (Δ1.7 ppm); mp 110–120 °C. ^2H NMR spectroscopy was performed by dissolving compound **23** (12 mg) in 1 mL of a solution of $CDCl_3$–$CHCl_3$ (0.5 to 4.5 mL) and two broad peaks were observed corresponding to the two deuteriums incorporated at C-3 with the following chemical shifts: δ 1.89 and 1.79.

X-ray Crystallography of Compound 28. Single crystals of compound **28** were prepared by slow evaporation of 2 mL of a solution of **28** in 1:1 EtOAc–hexanes, v/v, which was left to stand overnight. Suitable colorless plate-like crystals for compound **28** with dimensions of 0.30 mm × 0.24 mm × 0.17 mm were mounted in Paratone oil onto a nylon loop. All data were collected at 98(2) K, using a Rigaku AFC12/Saturn 724 CCD fitted with Mo Kα radiation (λ = 0.710 75 Å). Data collection and unit cell refinement were performed using CrysAlisPro software.[22] The total number of data were measured in the range 5.57° < 2θ < 55.0°, using ω scans. Data processing and absorption correction, giving minimum and maximum transmission factors (0.9635, 1.000), were accomplished with CrysAlisPro[23] and SCALE3 ABSPACK,[23] respectively. The structure, using Olex2,[24] was solved with the ShelXT[25] structure solution program using direct methods and refined (on F^2) with the ShelXL[26]

DOI: 10.1021/acs.jnatprod.9b00686
J. Nat. Prod. XXXX, XXX, XXX–XXX

refinement package using full-matrix, least-squares techniques. All non-hydrogen atoms were refined with anisotropic displacement parameters. All carbon-bound H atom positions were determined by geometry and refined by a riding model. The oxygen-bound H atom position was determined by electron density plot.

X-ray Crystallography of Compound 32. Single crystals of $C_{15}H_{24}O$ (compound **32**, diene) was prepared by slow evaporation of 2 mL of a solution of **32** in 1:1 MeOH−acetone, v/v, which was left to stand overnight. Suitable colorless plate-like crystals for compound (**32**) with dimensions of 0.33 mm × 0.30 mm × 0.13 mm were mounted in Paratone oil onto a nylon loop. All data were collected at 100(2) K, using a Rigaku AFC12/Saturn 724 CCD fitted with Mo Kα radiation (λ = 0.710 75 Å). Data collection and unit cell refinement were performed using CrysAlisPro software.[22] The total number of data were measured in the range 4.46° < 2θ < 52.0°, using ω scans. Data processing and absorption correction, giving minimum and maximum transmission factors (0.9733, 1.000), were accomplished with CrysAlisPro[23] and SCALE3 ABSPACK,[23] respectively. The structure, using Olex2,[24] was solved with the ShelXT[25] structure solution program using direct methods and refined (on F^2) with the ShelXL[26] refinement package using full-matrix, least-squares techniques. All non-hydrogen atoms were refined with anisotropic displacement parameters. All carbon-bound H atom positions were determined by geometry and refined by a riding model. The oxygen-bound H atom position was determined by electron density plot.

■ ASSOCIATED CONTENT

Supporting Information

The Supporting Information is available free of charge at https://pubs.acs.org/doi/10.1021/acs.jnatprod.9b00686.

1D NMR and IR spectra of **26**−**34** and **23**, HRMS spectra of **26**, **28**−**34**, and **23**, crystallographic data for diol **28** and diene **32**, and optimization conditions for **23** to **24** (time course, Table S1) (PDF)

X-ray data for diol **28** (CIF)

X-ray data for diene **32** (CIF)

■ AUTHOR INFORMATION

Corresponding Author

*E-mail: francis.yoshimoto@utsa.edu.

ORCID

Francis K. Yoshimoto: 0000-0002-2308-2999

Notes

The authors declare no competing financial interest.

■ ACKNOWLEDGMENTS

This research was generously supported by the Bill & Melinda Gates Foundation [OPP1188432] and startup funds from UTSA. The research was also supported from the UTSA NIH RISE Program (GM060655). A National Science Foundation Major Research Instrumentation grant (award number: 1625963) to support NMR facilities is acknowledged. We are grateful to Dr. Trevor Laird for helpful advice and comments.

■ REFERENCES

(1) Wang, J.; Xu, C.; Liao, F. L.; Jiang, T.; Krishna, S.; Tu, Y. *N. Engl. J. Med.* **2019**, *380*, 2087−2089.

(2) Wallaart, T. E.; Van Uden, W.; Lubberink, H. G. M.; Woerdenbag, H. J.; Pras, N.; Quax, W. J. *J. Nat. Prod.* **1999**, *62*, 430−433.

(3) Hang, Y.-S.; Liu, B.-Y.; Li, Z.-Q.; Ye, H.-C.; Wang, H.; Li, G.-F.; Han, J.-L. *Acta Bot. Sin.* **2004**, *46*, 1338−1346.

(4) Bryant, L.; Flatley, B.; Patole, C.; Brown, G. D.; Cramer, R. *BMC Plant Biol.* **2015**, *15* (175), 1−13.

(5) Soetaert, S. S. A.; Van Neste, C. M. F.; Vandewoestyne, M. L.; Head, S. R.; Goossens, A.; Van Nieuweburgh, F. C. W.; Deforce, D. L. D. *BMC Plant Biol.* **2013**, *13*, 220.

(6) Sy, L.-K.; Brown, G. D. *Tetrahedron* **2002**, *58*, 897−908.

(7) Brown, G. D.; Sy, L.-K. *Tetrahedron* **2004**, *60*, 1125−1138.

(8) Levesque, F.; Seeberger, P. H. *Angew. Chem., Int. Ed.* **2012**, *51*, 1706−1709.

(9) Triemer, S.; Gilmore, K.; Vu, G. T.; Seeberger, P. H.; Seidel-Morgenstern, A. *Angew. Chem., Int. Ed.* **2018**, *57*, 5525−5528.

(10) Amara, Z.; Bellamy, J. F. B.; Horvath, R.; Miller, S. J.; Beeby, A.; Burgard, A.; Rossen, K.; Poliakoff, M.; George, M. W. *Nat. Chem.* **2015**, *7*, 489−495.

(11) Wallaart, T. E.; Pras, N.; Quax, W. J. *J. Nat. Prod.* **1999**, *62*, 1160−1162.

(12) Roth, R. J.; Acton, N. *J. Nat. Prod.* **1989**, *52*, 1183−1185.

(13) Acton, N.; Roth, R. J. *J. Org. Chem.* **1992**, *57*, 3610−3614.

(14) Acton, N. *J. Nat. Prod.* **1999**, *62*, 790−793.

(15) Turconi, J.; Griolet, F.; Guevel, R.; Oddon, G.; Villa, R.; Geatti, A.; Hvala, M.; Rossen, K.; Goller, R.; Burgard, A. *Org. Process Res. Dev.* **2014**, *18*, 417−422.

(16) Dudley, G. B.; Engel, D. A.; Ghiviriga, I.; Lam, H.; Poon, K. W. C.; Singletary, J. A. *Org. Lett.* **2007**, *9*, 2839−2842.

(17) Elmarakby, S. A.; El-Feraly, F. S.; Elsohly, H. N.; Croom, E. M.; Hufford, C. D. *Phytochemistry* **1988**, *27*, 3089−3091.

(18) Zhu, J.-H.; Yu, R.-M.; Yang, L.; Hu, Y.-S.; Song, L.-Y.; Huang, Y.-J.; Li, W.-M.; Guan, S.-X. *Process Biochem.* **2010**, *45*, 1652−1656.

(19) Cunningham, I. M.; Overton, K. H. *J. Chem. Soc., Perkin Trans. 1* **1974**, *21*, 2458−2462.

(20) Schwertz, G.; Zanetti, A.; de Oliveira, M. N.; Fernandez, M. A. G.; Dioury, F.; Cossy, J.; Amara, Z. *Tetrahedron* **2019**, *75*, 743−748.

(21) Westheimer, F. H. *Chem. Rev.* **1961**, *61*, 265−273.

(22) *CrysAlisPro 1.171.38.41*; Rigaku, 2015.

(23) *SCALE3 ABSPACK*; Oxford Diffraction Ltd., 2005.

(24) Dolomanov, O. V.; Bourhis, L. J.; Gildea, R. J.; Howard, J. A. K.; Puschmann, H. *J. Appl. Crystallogr.* **2009**, *42*, 339.

(25) Sheldrick, G. M. *Acta Crystallogr., Sect. A: Found. Adv.* **2015**, *A71*, 3−8.

(26) Sheldrick, G. M. *Acta Crystallogr., Sect. A: Found. Crystallogr.* **2008**, *A64*, 112−122.

DOI: 10.1021/acs.jnatprod.9b00686
J. Nat. Prod. XXXX, XXX, XXX−XXX